Petroleum and Coal

Article **Open Access**

CHARACTERIZATION OF PORE SYSTEM CHANGES INDUCED BY DISSOLUTION IN CARBONATE ROCKS

Spariharijaona Andriamihaja, E. Padmanabhan*

Department of Geosciences, Faculty of Geosciences and Petroleum Engineering, Universiti Teknologi PETRONAS, 32610 Tronoh, Malaysia

Received June 18, 2017; Accepted September 22, 2017

Abstract

The influence of dissolution on pore development and its stability in carbonate rocks is crucial for EOR method. This study is aimed at enhancing the understanding of effect of dissolution on pore development in limestone. Dissolution experiments were conducted under laboratory controlled conditions and pore variations pre and post dissolution are compared using micro Computed Tomography (µCT scan) and SEM. Stability of pores in limestone is controlled by crystal size, crystal shape, percentage of pore surface in contact with pore fluids as well as microfossils. The results show that each individual pore reacts differently with the acid. Each pore develops in one or several stages including complete dissolution of materials at the pore wall, and enlargement of the pores (by 1.4 to 4.4 times). The pore enlargement decreases as the acid percolates within pores. Pore wall stability can be quantified by "rate of pore enlargement (RPE)" which is the area of pore enlargement variation over the dissolution time. The increment of pore lengths is function of fluid saturation and pore composition. Dissolution may apparently reduce pore size depending on the initial pore size at the surface. Throughout the experiments, dissolution process does not create any new pore systems. However, pores which have been previously hidden by matrix at the surface, become more opened and exposed after dissolution.

Keywords: pore wall; stability; carbonate rocks; dissolution; pore development.

1. Introduction

Changes of carbonate pore network by dissolution process is the key concept developed in Enhanced Oil Recovery (EOR) program [1-3], as well as Carbon Capture Storage (CCS) [4]. Chemical interaction between mineral and the reactive fluid often results to changes of pore network that lead to variation of fluid transport properties such as pore throat size, porosity, permeability and reactive surface area at macroscale [5-6]

Dissolution, responsible of these changes, is controlled by several factors such as temperature, pressure, pH [7-11]. Carbonate rock properties such as initial porosity, permeability, crystal size and mineralogical composition also control dissolution process [12-14].

µCT scan is now widely used to investigate the 3D internal structures of the rocks at high resolution [15-19]. The pore structure of the rock can then be characterized from the 3D pore network reconstruction attributes such porosity distribution, pore size, pore throat size and length and coordination number [20-23 Many published researches have addressed µCT scan as tool to evaluate the development of internal microstructure of the rock, as well as porosity, and permeability changes induced by dissolution [6,24-25].

Nur *et al.* [25] have investigated porosity, permeability variations due to the injection of carbon dioxide into carbonate rocks. They concluded that permeability changes were not in line with porosity change due to the displacement of fine particles. Nogues *et al.* [26] have analysed the evolution of porosity and permeability induced by dissolution. They found that the extensive increase of permeability is related to high concentrations of carbonic acid and not

related to pH, nor calcite saturation. Substantial porosity changes and relatively small permeability changes are caused by diffusive – dominated dissolution reaction near the inlet.

The advective transport system results to a large permeability changes for the same extent porosity. Yasuda *et al.* [27] investigate the effects of dissolution kinetics on porosity and permeability by injecting carbon dioxide into carbonate rocks. Their results revealed that only 1% weight loss of carbonate mass can increase the porosity and permeability by 50% and 180% respectively. Menke *et al.* [28] evaluated the impact of flow and pore structure of carbonate rocks on the chemical interaction between rock and acidic brine using X- Ray micro tomography (μCT scan). Their results show that at high flow rates, wormhole is created for heterogeneous carbonate and uniform dissolution for homogeneous carbonate. At low flow rates, dissolution is dominant nearer to the sample inlets for both carbonate rock types. Previous studies have been mainly focused on porosity and permeability changes induced by dissolution. However, pore wall stability of carbonate rocks which controls fluid flow, in response to dissolution, have not received much attention yet. The aim of this paper is to investigate the 3D pore system variations induced by dissolution and stability of pore structures.

2. Materials and methods

Carbonate rock compositions were evaluated using polarized microscope and Scanning Electron Micro-scope (SEM) operated at 3 KeV and with current varying from 1pA to 10nA. This evaluation consists of identification of different grains association, matrix and pore system (pore types, porosity).

Three porous carbonate rocks collected from Sarawak, Malaysia are used for dissolution experiment. These carbonate rocks are defined as boundstone rock, and have already been described in Andriamihaja, et al. [12] published work. Under controlled conditions, sample is placed in reactor chamber filled with 3 liters of diluted HCl of 0.1Molar. Dissolution experiment was performed at constant continuous stirrer rotation of 120 rpm with pH maintained at 1.2 and temperature sets at 75°C. An aliquant was collected every 10 minutes and then subsequently analyzed by Inductively Coupled Plasma Optical Emission Spectrometry (ICP-OES) to estimate [Ca^{2+}] released during the dissolution experiment. The dissolution rate for each sample at different temperature was deduced from the variation of [Ca^{2+}] during the experiment. X-Ray Ct scan images were used to evaluate the pore systems variations caused by dissolution at 75°C. Pores were randomly selected and pore imaging was done before and after dissolution.

3. Results and discussions

3.1. Pore changes

Analysis of the pores before and after dissolution shows that each pore has been enhanced by the dissolution as more pores are developed along an arbitrary z-axis after dissolution. The used acid in the dissolution first attacks the edges of the samples, eroding both matrix and grains leading to porosity enhancement (Figure 1b & d).

At the centre of the slice where acid reacts with the sample along an arbitrary z-axis, initial pores are enhanced but no new pores are formed. These pores increase in size, especially the intrafossil pores (Figure 1a&b). This implies that pore stability depends on the pore filling and pore wall (intrafossil) materials. Therefore, these materials dissolve faster than the matrix leading to instability of the pore system (Figure 1b &d). From X- ray CT scan images, these pore filling materials with dark gray colour exhibit lower density than the materials constituting the matrix. In order to further investigate the impact of dissolution on pore development, two pores (Pore A and Pore B) that reacted differently with the acid are selected and analyzed (Figure 1a & c).

The spatial development of the pore diameter in pore A with the percolation of acid can be subdivided into three main stages (Figure 2a). The first stage occurs within the first 50μm, where the material making up the pore are completely dissolved. The second stage (50μm to 675 μm) of the pore development corresponds to the pore enlargement stage. It is the stage

where the dissolution process is most active and the pore is enlarged by as much as 0.01 μm to 0.17 μm with a mean of 0.074 μm (std: 0.05). The pore sizes, therefore, increase by 1.13% to 25%. This pore enlargement process decreases as the acid percolates deeper within the pore. The last stage of the pore size development (from 675 μm to 1000 μm) is where the dissolution rate is reduced. Only slight and sporadic variations in the pores are observed at this stage. This observation is attributed to saturation of the acid by Ca and Mg ions as the dissolution process progresses and to the resistance of some carbonate crystals to dissolution.

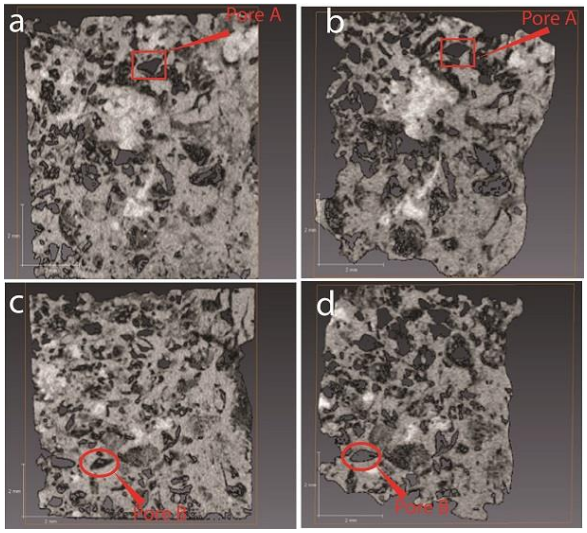

Figure 1. a) slice from CT scan images showing pore A (in rectangle) before dissolution experiment and the density variation of each components constituting the boundstone. The dark gray color is component with low density. b) Slice from CT scan images showing enhancement of pore A (in rectangle) after dissolution. c) Slice from CT scan images showing pore B (in circle) before dissolution experiment. d) Slice from CT scan images showing pore B (in circle) after dissolution

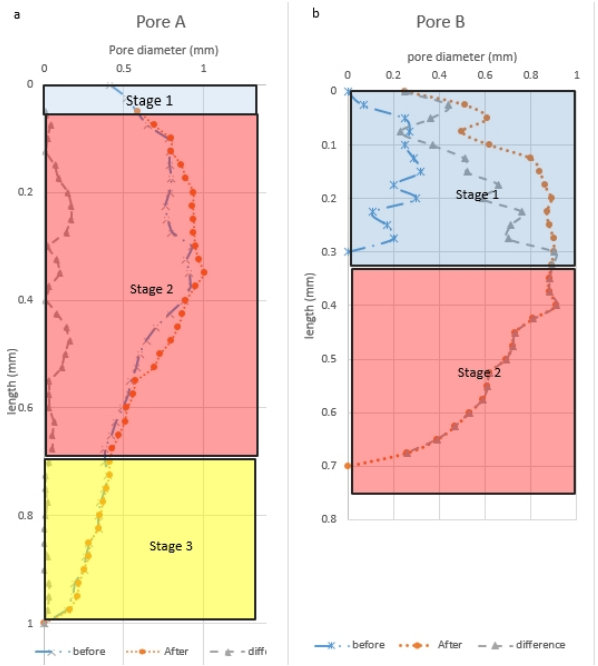

Figure 2. a) Pore size variation with pore length of pore A before (square plot), after dissolution (round plot) and the difference between pore size after and before dissolution along an arbitrary z- axis. b) Pore size variation with pore length of pore B before (square plot), after dissolution (round plot) and the difference between pore size after and before dissolution (triangle plot) along an arbitrary z- axis

In the second stage of the pore development, the dissolution process continues as long as the acid is not saturated and percolates deeper. This stage corresponds to pore diameter enlargement associated with pore length increment. Therefore, in this stage, pore diameter has been enlarged by 0.26 μm to 0.9 μm and decrease with depth, whiles the pore length has increased from 300 μm (before dissolution) to 700 μm (after dissolution). This implies that the pore has developed both laterally (increase in pore diameter) and vertically (increase in pore length). Therefore pore B is less stable than pore A.

3.2. Pore Wall Stability

One of the important factors controlling the pore wall stability is the carbonate crystals showing the highest surface area in contact with the pore fluids. These crystals dissolve faster than the crystals in lesser contact with the fluid. Another important factor to be considered is the crystal size. The smaller the crystal size, the higher the dissolution which in turn increases the instability of the pores. The crystal shape also has a significant effect on the pore wall stability. The rhombic crystals dissolve faster than the rounded crystals. Figure 3a illustrates that before dissolution carbonate crystals making up the pore wall are generally euhedral to subhedral (idiotopic to hypidiotopic fabric) before dissolution. They become more rounded (xenotopic crystal fabric) after dissolution (Figure 3b). Therefore, consequently, the pore wall after dissolution tends to be smoother. This implies that the stability of the pore wall is controlled by the initial shape of carbonate crystal constituting the pore wall.

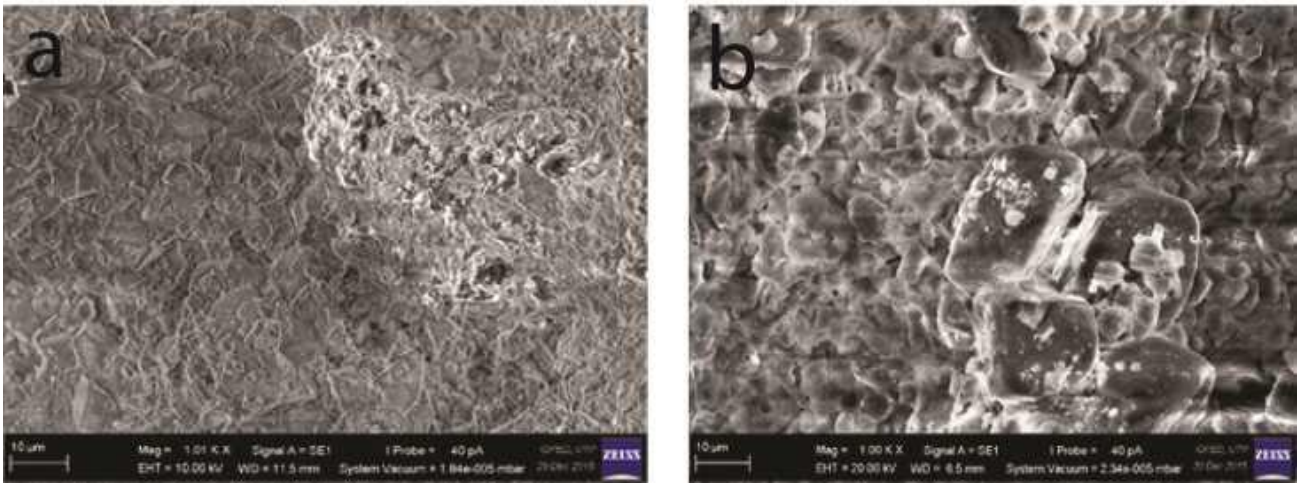

Figure 3. a) Idiotopic crystal fabric around the pore at surface before dissolution; b) rounded crystal after dissolution

Table 1. Pore size before and after dissolution

Pore size variation at 75°C (μm^2)	Before dissolution	After dissolution	Ratio	Impact of dissolution
Pore 1	175 066	244 833	1.4	Direct Enlargement
Pore 2	16 566	33 660	2	Direct Enlargement
Pore 3	2 100	9 200	4.4	Direct Enlargement
Pore 4	3 065	8 933	2.9	Direct Enlargement
Pore 5	16 064	8 733	0.5	Complete dissolution of pore around the surface/ Apparent pore size reduction
Pore 6	21944	16200	0.7	Complete dissolution of pore around the surface/ Apparent pore size reduction
Pore 7	-	85800	-	Apparent new pore
Pore 8	-	2688	-	Apparent new pore

As it has been reported earlier in the study of Andriamihaja *et al.* [12]at the initial stage of dissolution there is rapid increase of the released of [Ca^{2+}] which gradually slows with time. This rapid dissolution corresponds to three different type of pore developments after dissolution, occurring around the surface of the rock as illustrated in Figure 4:(1) direct enlargement of exposed pore at surface, (2) complete dissolution of pore around the surface (3) pore exposure associated with enlargement. The analysis of pore change around the surface of the rock samples are presented in table 1.

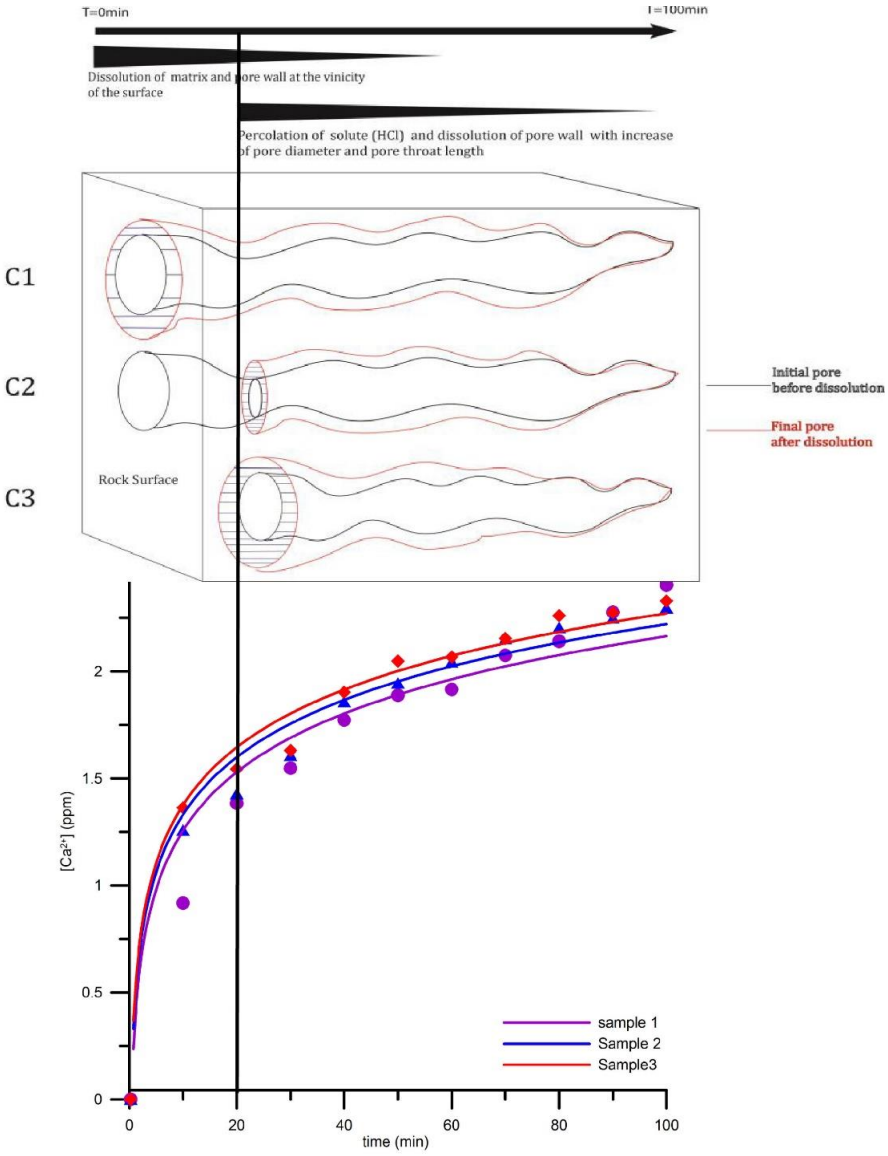

Figure 4. sketch showing 3 different cases of pore development induced by dissolution represented by: case 1 (C1), direct enlargement of pores exposed at rock surface; case 2 (C2) complete dissolution of pore at the vicinity of the rock surface; case 3 (C3) pore exposure associated with enlargement after dissolution

Direct pore enlargement at the rock surface

It corresponds to case1 (Figure 4). Pore enlargement corresponds to an enhancement of pore size directly in contact with diluted HCl. To properly visualize the pore enlargement process, four pores (pores 1 to 4) were randomly selected in order to compare their sizes before (Figure 5a) and after dissolution (Figure 5b). Each pore increases by 14 to 44 %

compared to the initial size (table 1). Analysis of the enlarged pores after dissolution shows that each pore develops differently during dissolution. Three possible scenarios can account for the variation in the development of each pore.

The first possibility involves pores that are smaller at the surface but larger at the base prior to dissolution. As the dissolution progresses, shallow materials controlling the pore sizes are dissolved and the larger pores emerge. Instability of the material making up the pore wall can also result in enlargement of the pores. The enlargement occurs when crystals at the pore walls are more soluble than the pore-fill material. Therefore as HCl percolates through the pore system, the carbonate minerals constituting the pore walls dissolve faster resulting in an increase of the pore sizes. The final scenario in the pore enlargement process may be due to a combination of the two possibilities described above. The pores enlarged from a combination of these two processes are characterized by lateral and vertical pore size variations (pore enlargement in two directions).

Pore wall stability can be quantified by "rate of pore enlargement (RPE)" and expressed by pore area variation over dissolution time (eq 1).

$$RPE = \frac{A_f - A_i}{\Delta t} \qquad (eq.1)$$

where :RPE: rate of pore enlargement [μm^2/min]; A_f: pore area after dissolution [μm^2]; A_i: pore area before dissolution [μm^2]; Δt: Dissolution time [min].

The higher the RPE is, the less stable the pore. In this study, the average RPE is 249.6 μm^2 /minute (μm^2/min). Pore 1 is the least stable pore with RPE of 697.67 μm^2/min and pore 4 is the most stable pore with RPE of 58.68 μm^2/min.

- ***Complete dissolution of pore around the surface***

It corresponds to case2 (Figure 4). Unlike in pores 1 to 4, pores 5 and 6 appear to have experienced a reduction in pore sizes after dissolution (Figure 5a and b). However, in reality, the larger pores initially at the surface prior to dissolution have been dissolved resulting in the emergence of smaller pores at the surface. These smaller pores were existent at the base prior to dissolution but have only become conspicuous after dissolution making it appear as if the pores sizes of pores 5 and 6 have been reduced by 0.5 and 0.7 from their initial sizes respectively.

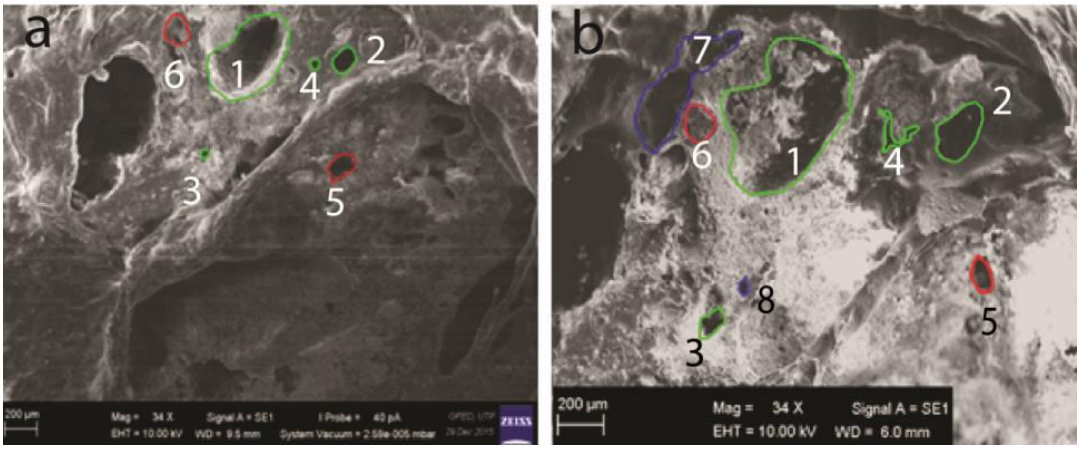

Figure 5. a) SEM of pores before dissolution, b) SEM of pore after dissolution at 75°C, pore size increasing (green), pore size decreasing (red), apparition of new pores (blue)

- ***Apparent new pores formation (exposure of pore initially covered)***

It corresponds to case 3 (Figure 4). Another effect of dissolution on the pores in the studied samples is the emergence of pores which were previously covered by crystals constituting the matrix and grains. The dissolution process removes the material covering these pores thereby exposing them and making it appear as if new pores have been created. This phenomenon is observed in pores 7 and 8 (Figure 5b).

4. Conclusion

This study seeks to understand the effect of dissolution on pore system developments and pore wall stability in carbonate rocks. The stability of pores in carbonate rocks is controlled predominantly by cement fabric. The important factors controlling the stability of pores in the studied samples include crystal size, crystal shape, and percentage of pore surface in contact with pore fluids, as well as the composition of microfossils.

Analysis of individual pores suggest that each single pore within the rocks behave differently during dissolution. The development of each pore system can be subdivided in several stages, based on response of the pore to percolating acid solution and the characteristic of carbonate materials at the pore wall and filling the pores. The dissolution process has three main effects on pore variation. The first effect involves the complete dissolution of the material making up the pores. This mainly occurs at the edge of the sample and within the first 50μm. The second effect is the pore size enlargement. It corresponds to lateral development of the pores. The third effect of dissolution on the individual pores is the lateral and vertical enhancement of the pore system. This effect results in an increase in both the pore diameter and pore length. The pores become more stable when filling materials are more stable and the acid solution percolating through the pores tends to be more saturated.

Acknowledgments

This study is supported by Yayasan UTP grant awarded to E. Padmanabhan.

References

[1] Bazin B. From Matrix Acidizing to Acid Fracturing: A Laboratory Evaluation of Acid/Rock Interactions: SPE Production & Facilities, 2001; 16(1): 22–29.

[2] Knox JA and Ripley EH. Fracture Acidizing in carbonate Rock. Journal of Canadian Petroleum, 1979: 77–90.

[3] Mcleod HO. 1989, Significant Factors for Successful Matrix Acidizing. SPE 20155., in Centennial Symposium Petroleum Technology: p. 1–21, doi.org/10.2118/20155-MS.

[4] Menke HP, Bijeljic B, Andrew MG and Blunt MJ. Dynamic three-dimensional pore-scale imaging of reaction in a carbonate at reservoir conditions: Environmental Science and Technology, 2015; 49(7): 4407–4414.

[5] Luquot L and Gouze P. 2009, Experimental determination of porosity and permeability changes induced by injection of CO_2 into carbonate rocks. Chemical Geology, 2009; 265(1–2): 148–159.

[6] Noiriel C, Luquot L, Madé B, Raimbault L. Gouze P and van der Lee J. Changes in reactive surface area during limestone dissolution: An experimental and modelling study. Chemical Geology, 2009; 262(3–4): 353–363.

[7] Adham AKM and Kobayashi A. 2009, Effect of Intensity and pH of Rain on the Dissolution of Limestone. in Proceedings of the Nineteenth (2009) International Offshore and Polar Engineering Conference Osaka, Japan (Vol. 1, pp. 1196–1201).

[8] Crockford P, Telmer K and Best M. Dissolution kinetics of Devonian carbonates at circumneutral pH, 50bar pCO2, 105°C, and 0.4M: The importance of complex brine chemistry on reaction rates. Applied Geochemistry, 2014; 41: 128–134, doi:10.1016/j.apgeochem.2013.12.008.

[9] Dolgaleva IV, Gorichev IG, Izotov AD, Stepanov VM. Modeling of the Effect of pH on the Calcite Dissolution Kinetics. Theoretical Foundations of Chemical Engineering, 2005; 39(6): 614–621.

[10] Kirstein J, Hellevang H, Haile BG, Gleixner G and Gaupp R., 2016, Experimental determination of natural carbonate rock dissolution rates with a focus on temperature dependency. Geomorphology, 2016; 261: 30–40.

[11] Peng C, Crawshaw JP, Maitland GC and Trusler JPM. 2015, Kinetics of calcite dissolution in CO2-saturated water at temperatures between (323 and 373)K and pressures up to 13.8MPa. Chemical Geology, 2015; 403: 74–85.

[12] Andriamihaja S, Padmanabhan E and Ben-Awuah J. Characterization of pore systems in carbonate using 3D X -ray computed tomography: Pet Coal, 2016; 58(4): 507–516.

[13] Cohen CE, Ding D, Quintard M and Bazin B. From pore scale to wellbore scale: Impact of geometry on wormhole growth in carbonate acidization. Chemical Engineering Science, 2008; 63(12): 3088–3099.

[14] Kalia N and Balakotaiah V., Effect of medium heterogeneities on reactive dissolution of carbonates. Chemical Engineering Science, 2009; 64(2): 376–390.
[15] Arns CH, Bauget F, Limaye A, Sakellariou A, Senden TJ. Sheppard AP, Øren P. 2004. Pore Scale Characterisation of Carbonates using X-ray microtomography. In SPE International (Ed.), SPE Annual Technical Conference and Exhibition. Houston.
[16] Berg S, Ott H, Klapp SA, Schwing A, Neiteler R, Brussee N, Makuraa A, Leua L, Enzmann F, Schwarz J-O, Kersten M, Irvine S and Stampanoni M. Real-time 3D imaging of Haines jumps in porous media flow. in Proceedings of the National Academy of Sciences of the United States of America: p. 3755–9, doi:10.1073/pnas.1221373110.
[17] Blunt MJ, Bijeljic B, Dong H, Gharbi O, Iglauer S, Mostaghimi P, Paluszny A and Pentland C. Pore-scale imaging and modelling. Advances in Water Resources, 2013; 51: 197–216,
[18] Knackstedt MA, Arns CH, Bauget F, Sakellariou A, Senden TJ, Sheppard AP and Sok RM., 2006, QUANTITATIVE TRANSPORT PROPERTIES OF GRANULAR MATERIAL CALCULATED FROM X-RAY μCT IMAGES: *International Petroleum Conference and Exhibition (Petrotech-2005)*, Society of Petroleum Engineers, USA: 92–97.
[19] Wildenschild, D and Sheppard AP. X-ray imaging and analysis techniques for quantifying pore-scale structure and processes in subsurface porous medium systems. Advances in Water Resources, 2013; 51: 217–246.
[20] Andriamihaja S, Padmanabhan E, Ben-Awuah J and Sokkalingam R. 2016, Modeling the impacts of petrophysical and textural parameters on dissolution of carbonate rocks at 25°C, 50°C, and 75°C. Pet Coal, 2016; 58(3): 359-367.
[21] de Boever E, Varloteaux C, Nader FH, Foubert A, Békri S, Youssef S and Rosenberg E. Quantification and Prediction of the 3D Pore Network Evolution in Carbonate Reservoir Rocks. OGST - Revue d'IFP Energies nouvelles, 2012; 67(1): 161–178.
[22] Dong H, Touati M and Blunt M. 2007, Pore network modeling: analysis of pore size distribution of Arabian core samples, in SPE Middle East Oil & Gas Show and Conference: doi:10.2523/105156-MS.
[23] Freire-Gormaly M, Ellis JS, MacLean HL and Bazylak A. 2015, Pore Structure Characterization of Indiana Limestone and Pink Dolomite from Pore Network Reconstructions. OGST - Revue d'IFP Energies nouvelles, 2015; 71(3):1-14 doi:10.2516/ogst/2015004.
[24] Rötting TS, Luquot L, Carrera J and Casalinuovo DJ. Changes in porosity, permeability, water retention curve and reactive surface area during carbonate rock dissolution. Chemical Geology, 2015; 403: 86–98.
[25] Nur A, Vanorio T, Diaz E, Stanford T and Physics R. 2011, Effects of Carbon Dioxide Injection in Reactive Carbonates : Computational Rock Physics Basis for Time-Lapse Monitoring, in SPE/DGS Saudi Arabia Section Technical Symposium and Exhibition: p. 1–6, doi:https://www.onepetro.org/conference-paper/SPE-149065-MS.
[25] Qajar J, Francois N, Arns ChH. Microtomographic Characterization of Dissolution-Induced Local Porosity Changes Including Fines Migration in Carbonate Rock, SPE J., 2013; 18(03):545-562.
[26] Nogues JP, Fitts JP, Celia MA and Peters CA. Permeability evolution due to dissolution and precipitation of carbonates using reactive transport modeling in pore networks: Water Resources Research, 2013; 49(9):, 6006-6021.
[27] Yasuda EY, dos Santos RG and Trevisan OV. Kinetics of carbonate dissolution and its effects on the porosity and permeability of consolidated porous media. Journal of Petroleum Science and Engineering, 2013; 112: 284–289.
[28] Menke H, Bijeljic B, Andrew MG and Blunt MJ. Dynamic pore-scale imaging of reactive transport in heterogeneous carbonates at reservoir conditions. Energy Procedia, 2014; 63: p. 5503–5511.

To whom correspondence should be addressed: Dr. Spariharijaona Andriamihaja, Department of Geosciences, Faculty of Geosciences and Petroleum Engineering, Universiti Teknologi PETRONAS, 32610 Tronoh, Malaysia, andriamis@yahoo.fr